Turing Models for Spatial Pattern Formation

B5.5 Further Mathematical Biology

Candidate Number: 1020036

1 Introduction

The study of pattern formation has been fundamental to developmental biology. Most of the research in the field is concerned with determining the mechanisms that generate patterns and forms in early development. The application of mathematical modelling has played an important role in studying and predicting biological patterns, and most of the models have similar patterning mechanisms of short-range activation and long-range inhibition. In this paper, we study the Turing model, which is the most well-known model in the study of patterns and forms. Turing's theory of pattern formation states that diffusing and reacting chemicals, under certain conditions, produce spatially heterogeneous patterns from initial uniform states. The spatially heterogeneous chemical concentrations create different levels of growth and cause a change in morphology [3, p373-374]. The equations for reaction-diffusion mechanisms take the form:

$$\frac{\partial \mathbf{u}}{\partial t} = \mathbf{D}\nabla^2\mathbf{c} + \mathbf{f}(\mathbf{u})$$

where $\mathbf{u}$ denotes the vector of morphogen concentrations, $\mathbf{f}$ denotes the reaction kinetics, and $\mathbf{D}$ is the diagonal matrix of constant diffusion coefficients.

In the absence of diffusion (namely, $\mathbf{D} = \mathbf{0}$), the chemical concentrations tend to a linearly stable uniform steady state and small random perturbations produce spatially inhomogeneous patterns by diffusion-driven instability. The idea is novel because people usually consider diffusion as a stabilising process [3, p375].

In this paper, we study Turing models with two chemical species and Schnakenberg reaction kinetics on one-dimensional and two-dimensional domains. We numerically solve the reaction-diffusion systems and investigate the influence of domain size and shape on the generation of spatial patterns.

2 Derivation of reaction-diffusion equations

Let us consider a reaction-diffusion model with two chemicals, namely $u(\mathbf{x}, t)$ and $v(\mathbf{x}, t)$. Let $\mathbf{u} = (u(\mathbf{x}, t), v(\mathbf{x}, t))^T$, where $u(\mathbf{x}, t)$ and $v(\mathbf{x}, t)$ denote the concentrations of the chemicals at position $\mathbf{x}$ and time t, and $\mathbf{x} \in \Omega$ and $t \in [0, \infty]$. Note that Ω is a simply connected and bounded domain in $\mathbb{R}^2$.

We follow the paper by Madzvamuse [1, p11-13] to derive reaction-diffusion equations on a fixed domain. By the Law of Mass Balance, the rate of change of a chemical in Ω is equal to the sum of the net flux of the chemical through the boundary $\partial\Omega$ and the net production of the chemical within the domain. Let $\mathbf{F} = (F1, F2)^T$ denote the chemical fluxes of u and v per unit area, respectively, and $\mathbf{f} = (f, g)^T$ denote the net production rates per unit volume. Then, we have

$$\frac{d}{dt}\int_\Omega \mathbf{u}\ \mathrm{d}\Omega = -\int_{\partial\Omega} F \cdot \mathrm{d}\mathbf{S} + \int_\Omega \mathbf{f}(\mathbf{u})\ \mathrm{d}\Omega \tag{1}$$

Assuming that $\mathbf{u}$ is continuous, by Divergence Theorem, we can rewrite (1) as the fol-

lowing equation:

$$\int_\Omega \frac{\partial \mathbf{u}}{\partial t} + \nabla \cdot \mathbf{F} - \mathbf{f}(\mathbf{u}) \, \mathrm{d}\Omega = 0 \tag{2}$$

According to Fick's Law of Diffusion, the flux $\mathbf{F}$ and the gradient of $\mathbf{u}$ satisfy the relation:

$$\mathbf{F} = -\mathbf{D}\nabla\mathbf{u} \tag{3}$$

where $\mathbf{D}$ is the matrix of diffusion coefficient independent of $\mathbf{F}$ and $\nabla\mathbf{u}$.

Thus, combining (2) and Fick's Law, we end up with a system of reaction-diffusion equations for two chemical species u and v in the bounded domain Ω:

$$\frac{\partial \mathbf{u}}{\partial t} = \mathbf{D}\nabla^2\mathbf{u} + \mathbf{f}(\mathbf{u}) \tag{4}$$

where $\mathbf{D}$ takes the form

$$\mathbf{D} = \begin{bmatrix} D_1 & 0 \\ 0 & D_2 \end{bmatrix}.$$

Note that initial conditions and boundary conditions for u and v also need to be included.

2.1 Nondimensionalisation

For nondimensionalisation, we define the following scaling parameters:

$$T = \frac{{L_x}^2}{D_1}, \quad \gamma = \frac{k_2 {L_x}^2}{D_1}, \quad d = \frac{D1}{D2} \tag{5}$$

where L_x is the length scale, k_2 is a reaction kinetic rate [2, p509] . We set

$$\mathbf{u} = \mathbf{U}\tilde{\mathbf{u}}, \quad t = T\tau, \quad \mathbf{x} = L_x\tilde{\mathbf{x}} \tag{6}$$

and obtain the following dimensionless system

$$\frac{\partial \tilde{\mathbf{u}}}{\partial \tau} = \tilde{\mathbf{D}}\tilde{\mathbf{u}} + \gamma\mathbf{f}(\tilde{\mathbf{u}}), \tag{7}$$

where

$$\tilde{\mathbf{D}} = \begin{bmatrix} 1 & 0 \\ 0 & d \end{bmatrix}.$$

3 Diffusion-driven instability

In a reaction-diffusion model, Turing believed that spatial patterns can be produced via diffusion-driven instability which occurs when a stable homogeneous steady state solution in the absence of diffusion becomes unstable with diffusion present. For example, in the case of animal coat markings, the instability in the diffusion of morphogens results in the

patterning on animals' skins. Closely following the book by Murray [3, p380-386], here we derive the conditions for diffusion-driven instability for a reaction-diffusion system with zero flux boundary conditions via linear analysis.

3.1 Linear analysis

Consider a two-dimensional reaction-diffusion system with homogeneous Neumann boundary conditions:

$$\frac{\partial \mathbf{u}}{\partial t} = \mathbf{D}\nabla^2\mathbf{u} + \mathbf{F}(\mathbf{u}) \tag{8}$$

$$\mathbf{n}\cdot\nabla\mathbf{u} = 0, \quad \mathbf{x}\in\partial\Omega,$$

where

$$\mathbf{u} = \begin{bmatrix} u \\ v \end{bmatrix}, \quad \mathbf{D} = \begin{bmatrix} D_u & 0 \\ 0 & D_v \end{bmatrix}, \quad \text{and } \mathbf{F} = \begin{bmatrix} f(u,v) \\ g(u,v) \end{bmatrix}.$$

First, we linearise the equations. Let $\mathbf{u}^*$ be a vector that satisfies $\mathbf{F}(\mathbf{u}^*) = 0$ and let $\mathbf{w} = \mathbf{u} - \mathbf{u}^* \ll 1$. Then,

$$\frac{\partial \mathbf{w}}{\partial t} = \mathbf{D}\nabla^2\mathbf{w} + \mathbf{F}(\mathbf{u}^* + \mathbf{w}) \tag{9}$$

$$= \mathbf{D}\nabla^2\mathbf{w} + \mathbf{F}(\mathbf{u}^*) + \mathbf{J}_\mathbf{F}(\mathbf{u}^*)\mathbf{w} + o(\mathbf{w}^2), \tag{10}$$

where

$$\mathbf{J}_\mathbf{F}(\mathbf{u}^*) = \begin{bmatrix} f_u & f_v \\ g_u & g_v \end{bmatrix}(\mathbf{u}^*). \tag{11}$$

Ignoring the higher order terms, we obtain the following system of equations:

$$\frac{\partial \mathbf{w}}{\partial t} = \mathbf{D}\nabla^2\mathbf{w} + \mathbf{J}_\mathbf{F}\mathbf{w} \tag{12}$$

with $\mathbf{n}\cdot\mathbf{w} = 0,\ \mathbf{x}\in\partial\Omega$.

Second, we seek $\mathbf{w}$ in the form of a separable solution

$$\mathbf{w}(\mathbf{x},t) = A(t)\mathbf{p}(\mathbf{x}), \tag{13}$$

where

$$A(t) = A_0 e^{\lambda t}, \quad \lambda = \frac{A'}{A}, \quad A_0 \neq 0.$$

Substituting (13) into equation (12), we obtain the following equation

$$\lambda\mathbf{p} = \mathbf{D}\nabla^2\mathbf{p} + \mathbf{J}_\mathbf{F}\mathbf{p}. \tag{14}$$

Assuming that $\mathbf{p}$ satisfies the equation

$$\nabla^2 \mathbf{p} + k^2 \mathbf{p} = 0 \tag{15}$$

$$\mathbf{n} \cdot \mathbf{p} = 0, \quad \mathbf{x} \in \partial\Omega, \tag{16}$$

we can rewrite (14) as

$$(\lambda \mathbf{I} - \mathbf{J_F} + \mathbf{D}k^2)\mathbf{p} = 0. \tag{17}$$

For nontrivial solution, we require

$$\left|\lambda \mathbf{I} - \mathbf{J_F} + k^2 \mathbf{D}\right| = 0, \tag{18}$$

i.e.

$$\left| \begin{bmatrix} \lambda - f_u + D_u k^2 & -f_v \\ -g_u & -\lambda - g_v + D_v k^2 \end{bmatrix} \right| = 0, \tag{19}$$

which yields the following quadratic equation of λ:

$$\lambda^2 + ((D_u + D_v)k^2 - f_u - g_v)\lambda + D_v D_v k^4 - (D_v f_u + D_u f_v)k^2 + f_u g_v - g_u f_v. \tag{20}$$

Note that for any k^2 and $\mathbf{p}_k$ that satisfy equation (15), we have a separable solution in the form

$$A_0 e^{\lambda(k^2)t} \mathbf{p}_k(\mathbf{x}).$$

Recall that a diffusion-driven instability requires the homogeneous steady state to be stable in the absence of diffusion and unstable when diffusion is present. For the system to be stable without diffusion, we require $Re(\lambda(0)) < 0$, which implies $\mathbf{u}^*$ is linearly stable. So, we set $k^2 = 0$ to remove the diffusion term, and equation (20) yields

$$\lambda - (f_u + g_v)\lambda + (f_u g_v - g_u f_v) = 0, \tag{21}$$

which gives rise to the two conditions for stability without diffusion:

$$f_u + g_v < 0 \tag{22}$$

$$f_u g_v - g_u f_v > 0. \tag{23}$$

In addition, we require the system to be unstable with diffusion present. So, we need to show that there exists k^2 such that $Re(\lambda(k^2)) > 0$, which implies $\mathbf{u}^*$ is linearly unstable and the perturbation from the steady state will grow into a spatially heterogeneous solution and patterns will occur.

For $k^2 > 0$, (20) yields

$$h(k^2) = D_u D_v k^4 - (D_v f_u + D_u g_v)k^2 + (f_u g_v - g_u f_v) < 0. \tag{24}$$

Solving (24) for k^2, we find that instability occurs when

$$\frac{A - \sqrt{A^2 - B}}{2D_u D_v} < k^2 < \frac{A + \sqrt{A^2 - B}}{2D_u D_v}, \tag{25}$$

$$\tag{26}$$

where $A = D_v f_u + D_u g_v$, and $B = 4D_u D_v (f_u g_v - g_u f_v)$.

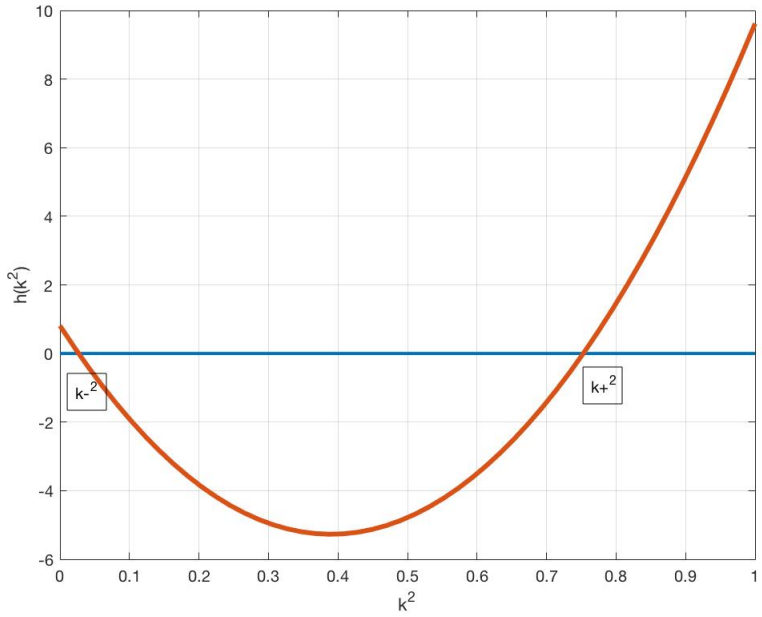

Figure 1: A plot of $h(k^2)$ based on Schnakenberg model

Figure (1) shows a plot of $h(k^2)$ based on Schnakenberg reaction-diffusion system, where instability exists when $k^2 \in [{k_-}^2, {k_+}^2]$.

Thus, (24) yields the two conditions for instability with diffusion:

$$D_v f_u + D_u g_v > 0 \tag{27}$$

$$(D_v f_u + D_u g_v) > 2\sqrt{D_u D_v (f_v g_v - f_v g_u)}. \tag{28}$$

To sum up, diffusion-driven instability occurs when conditions (22), (23), (27) and (28) are satisfied [3, p380-386].

4 Schnakenberg model

Schnakenberg model is a hypothetical Turing model, meaning that it is derived by assuming a hypothetical chemical reaction then obtaining corresponding reaction kinetics based on the Law of Mass Action. According to Ref. [1, p21], in 1979, Schnakenberg proposed a

series of hypothetical trimolecular autocatalytic reactions:

$$\mathrm{X} \underset{k_2}{\overset{k_1}{\rightleftharpoons}} \mathrm{A}, \mathrm{B} \xrightarrow{k_4} \mathrm{Y}, 2\mathrm{Y} + \mathrm{X} \xrightarrow{k_3} 3\mathrm{X}.$$

We denote the concentrations of X, Y, A, and B as u, v, a_1, and b_1 respectively and derive the reaction kinetics of X and Y using the Law of Mass Action, which are

$$\begin{aligned} f(u,v) &= k_1 a_1 - k_2 u + k_3 u^2 v \\ g(u,v) &= k_4 b_1 - k_3 u^2 v. \end{aligned}$$

To simplify the model, we assume that a_1 and b_1 remain constant. Then, the system can be nondimensionised in the following way:

$$\begin{aligned} \frac{\partial u}{\partial t} &= \gamma(a - u + u^2 v) + \nabla^2 u \\ \frac{\partial v}{\partial t} &= \gamma(b - u^2 v) + d\nabla^2 u, \end{aligned}$$

where

$$a = \frac{k_1 a_1}{k_2}\sqrt{\frac{k_3}{k_2}}, \quad b = \frac{k_4 b_1}{k_2}\sqrt{\frac{k_3}{k_2}}, \quad \text{and } \gamma = \frac{k_2 L_x^2}{D_1}.$$

Note that $d = D_2/D_1$, and parameters a, b and γ are positive. The term $u^2 v$ means the activation of u and consumption of v [1, p21-22].

4.1 One dimensional Schnakenberg model

Let us consider the following nondimensionalised Schnakenberg model in 1D:

$$u_t = \gamma(a - u + u^2 v) + u_{xx} \tag{29}$$
$$v_t = \gamma(b - u^2 v) + d v_{xx} \tag{30}$$

for $x \in [0, L]$, $t \in [0, \infty]$. And u, v satisfy homogeneous Neumann boundary conditions at $x = 0$ and $x = L$.

Note that the equation

$$p_{xx} + k^2 p = 0 \tag{31}$$
$$p'(0) = 0 = p'(L) \tag{32}$$

gives eigenfunction solutions

$$p_k(x) = A_k \cos(kx), \quad k = \frac{n\pi}{L}, \quad n = 1, 2, \cdots, \tag{33}$$

which leads to a separable solution in the form

$$p(x) = \sum_k A_k e^{\lambda(k^2)t} \cos(kx) \tag{34}$$

In addition, we notice that the Schakenberg system has one steady state in the absence of diffusion, which is given by

$$u^* = a + b, \quad v^* = \frac{b}{(a+b)^2}. \tag{35}$$

Applying the conditions of diffusion-driven instability on Schnakenberg model, we obtain the following restrictions on the parameters a, b and d:

$$f_u + g_v < 0 \implies 0 < b - a < (a+b)^3 \tag{36}$$

$$f_u g_v - f_v g_u > 0 \implies (a+b)^2 > 0 \tag{37}$$

$$df_u + g_v > 0 \implies d(b-a) > (a+b)^3 \tag{38}$$

$$(df_u + g_v)^2 - 4d(f_u g_v - f_v g_u) > 0 \implies (d(b-a) - (a+b)^3)^2 > 4d(a+b)^4. \tag{39}$$

The algebraic work above follows Ref. [3, p287]. We use conditions (36), (37), (38), and (39) to determine the values of parameters for the Schnakenberg model when conducting numerical simulations.

4.1.1 Domain size

According to Murray [3, p388], for the smallest value $k^2 = (\pi/L)^2$, as we recall from previous linear stability analysis (25), the condition for a diffusion-driven instability is

$$k_-{}^2 < k^2 = \frac{\pi^2}{L^2} < k_+{}^2,$$

where

$$k_-{}^2 = \frac{A - \sqrt{A^2 - B}}{2d}, \quad k_+{}^2 = \frac{A + \sqrt{A^2 - B}}{2d}.$$

Therefore, when the domain size L is so small that

$$k^2 = \frac{\pi^2}{L^2} > k_+{}^2,$$

diffusion-driven instability fails to occur, and patterns cannot be formed via Turing mechanism. However, as we increase the domain size L to a certain level so that $k^2 \in [k_-{}^2, k_+{}^2]$, the homogeneous steady state becomes unstable and results in pattern formation.

4.1.2 Numerical results

In this section, we used the finite element method introduced in the paper "A Numerical Approach to the Study of Spatial Pattern Formation" by Madzvamuse to solve the 1D Schnakenberg model proposed above [1, p41-68]. We first introduce the following function spaces for the variational formulations of the Schnakenberg problem:

$$L_2([0, L]) = \{v|\ v \text{ is defined on} [0, L], \text{and } \int_0^L v^2 \mathrm{d}x < \infty\} \tag{40}$$

$$H^1([0, L]) = L_2([0, L]) = \{v | v, v_x \in L^2([0, L])\} \tag{41}$$

Now, we reformulate the reaction-diffusion equations to its weak form: $\forall w \in H^1([0, L])$,

$$(u_t, w) = (\gamma(a - u + u^2 v), w) + (u_{xx}, w) \tag{42}$$

$$(v_t, w) = (\gamma(a - u^2 v), w) + (v_{xx}, w), \tag{43}$$

where

$$(u, v) = \int_0^L uv \ \mathrm{d}x.$$

Thus, solving the reaction-diffusion system is equivalent to solving the following problem: find $u, v \in H^1([0, L])$ such that $\forall w \in H^1([0, L])$,

$$(u_t, w) = (\gamma(a - u + u^2 v), w) - (u_x, w_x) \tag{44}$$

$$(v_t, w) = (\gamma(a - u^2 v), w) - d(v_x, w_x). \tag{45}$$

To solve the problem numerically, we reduce the number of degrees of freedom to a finite

level via method of discretization. Starting with a spatial discretization of the domain $[0, L]$, we let $0 = x_0 < x_1 < \cdots < x_M < x_{M+1} = L$ be a regular partition of $[0, L]$ and let each subinterval (x_{j-1}, x_j) have equal length $h = \frac{1}{M+1}$, where $j = 1, \cdots, M+1$.

Now, we define V_h to be a finite-dimensional subspace of $H^1([0, L])$ such that

$$V_h = \{v \in H^1([0, L]) | v \text{ is linear on } [x_{j-1}, x_j]\}$$

and introduce the basis functions of V_h, also known as linear shape functions, $\phi_1, \phi_2, \cdots, \phi_M$, which are defined as: $\forall\ j = 1, \cdots, M$

$$\phi_j(x_i) = \begin{cases} 1 & if\ i = j \\ 0 & if\ i \neq j \end{cases}.$$

In words, ϕ_j is a continuous piece-wise linear function that takes value 1 at point x_j and takes value 0 at x_i when $i \neq j$. Notice that every function $v_h \in V_h$ can be expressed in a unique way as a linear combination of the basis functions $\{\phi_i\}_{i=1}^{M}$. Thus, let u^h and v^h denote the finite element approximation of u and v such that

$$u^h(x, t) = \sum_{i=0}^{M+1} u_i(t)\phi_i(x) \tag{46}$$

$$v^h(x, t) = \sum_{i=0}^{M+1} v_i(t)\phi_i(x). \tag{47}$$

We replace u, v in equations (44) and (45) with u^h, v^h and replace test function w with $\phi_j,\ j = 0, \cdots M+1$, where $u, v, w \in H^1([0, L])$ and $u^h, v^h, \phi_j \in V^h,\ \forall j$. Then, we obtain the following system of equations

$$\partial_t(u^h, \phi_j) = (\gamma(a - u^h + (u^h)^2 v^h), \phi_j) - (\partial_x u, \partial_x \phi_j),\ j = 0, ..., M+1 \tag{48}$$

$$\partial_t(v^h, \phi_j) = (\gamma(a - (u^h)^2 v^h), \phi_j) - (\partial_x v, \partial_x \phi_j),\ j = 0, ..., M+1, \tag{49}$$

which can be written in matrix form

$$\mathbf{M}\frac{\mathrm{d}\mathbf{U}(t)}{\mathrm{d}t} = \gamma(a\mathbf{G} - \mathbf{M}\mathbf{U} + \mathbf{K}^1\mathbf{U}) - \mathbf{S}\mathbf{U} \tag{50}$$

$$\mathbf{M}\frac{\mathrm{d}\mathbf{V}(t)}{\mathrm{d}t} = \gamma(b\mathbf{G} - \mathbf{K}^2\mathbf{V}) - d\mathbf{S}\mathbf{U}, \tag{51}$$

where

$$\mathbf{M} = \begin{bmatrix} (\phi_0, \phi_0) & \cdots & (\phi_0, \phi_{M+1}) \\ \vdots & \ddots & \vdots \\ (\phi_{M+1}, \phi_0) & \cdots & (\phi_{M+1}, \phi_{M+1}) \end{bmatrix}, \mathbf{S} = \begin{bmatrix} (\partial_x\phi_0, \partial_x\phi_0) & \cdots & (\partial_x\phi_0, \partial_x\phi_{M+1}) \\ \vdots & \ddots & \vdots \\ (\partial_x\phi_{M+1}, \partial_x\phi_0) & \cdots & (\phi_{M+1}, \phi_{M+1}) \end{bmatrix}$$

$$\mathbf{U}(t) = \begin{bmatrix} u_0 \\ \vdots \\ u_{M+1} \end{bmatrix}(t),\ \mathbf{V}(t) = \begin{bmatrix} v_0 \\ \vdots \\ v_{M+1} \end{bmatrix}(t), \mathbf{G} = \begin{bmatrix} \int_0^L \phi_0 \ \mathrm{d}x \\ \vdots \\ \int_0^L \phi_{M+1} \ \mathrm{d}x \end{bmatrix},$$

and $\mathbf{K}^1, \mathbf{K}^2$ are the matrices obtained from the nonlinear terms in the equations. $\mathbf{K}^1$ is dependent on $\mathbf{U}, \mathbf{V}$ and $\mathbf{K}^2$ is dependent on $\mathbf{U}$.

Because of the uniform mesh we use for the spatial discretization, the global mass matrix $\mathbf{M}$, stiffness matrix $\mathbf{S}$ and global force vector $\mathbf{G}$ can be directly computed. We compute the nonlinear matrices $\mathbf{K}^1, \mathbf{K}^2$ by evaluating the element matrices exactly and then assembling the global matrices [1, p49-54].

For example, over subinterval $[x_l, x_{l+1}]$, the local nonlinear matrices K^1, K^2 of $\mathbf{K}^1, \mathbf{K}^2$, respectively, can be calculated as follows: for $i, j = 1, 2$,

$$K^1_{ij} = \int_{x_l}^{x_{l+1}} N_j N_i (u_l N_2 + u_{l+1} N_i)(v_l N_2 + v_{l+1} N_i) \mathrm{d}x, \tag{52}$$

$$K^2_{ij} = \int_{x_l}^{x_{l+1}} N_j N_i (u_l N_2 + u_{l+1} N_i)^2 \mathrm{d}x, \tag{53}$$

where

$$N_1(x) = \frac{x - x_l}{h}, \quad N_2(x) = \frac{x_{l+1} - x}{h} \quad [1, \text{p54-55}].$$

It is worth mentioning that the homogeneous Neumann boundary conditions are imposed by the variational formation automatically so there is no need to modify the matrices for boundary condition implementation.

Now, we apply backward Euler method to the systems of ODEs we obtain in (50) and (51):

$$(\mathbf{M} + \Delta t\gamma\mathbf{M} + \Delta t\mathbf{S})\mathbf{U}^{n+1} = \Delta\gamma a\mathbf{G} + \mathbf{M}\mathbf{U}^n + \Delta t\gamma\mathbf{K}^1\mathbf{U}^n \tag{54}$$

$$(\mathbf{M} + d\Delta t\mathbf{S})\mathbf{V}^{n+1} = \Delta\gamma b\mathbf{G} + \mathbf{M}\mathbf{V}^n - \Delta t\gamma\mathbf{K}^2\mathbf{V}^n, \tag{55}$$

where Δt is the time-step, and $\mathbf{U}^n = \mathbf{U}(n\Delta t), \mathbf{V}^n = \mathbf{V}(n\Delta t)$. Because backward Euler method is unconditionally stable, we are allowed to take relatively large time-step without compromising the stability of the numerical method. Notice that we use $\mathbf{U}^n, \mathbf{V}^n$ to compute the nonlinear matrices instead of $\mathbf{U}^{n+1}, \mathbf{V}^{n+1}$ so that the systems are linear and can be directly solved [1, p66-68].

For our numerical simulation, we let $a = 0.1, b = 0.9, d = 40$ so that the conditions for diffusion-driven instability ((22), (23), (27), (28)) are satisfied. For initial conditions, we

randomly perturb the steady state solutions

$$u^* = a + b = 1, \text{ and } v^* = \frac{b}{(a+b)^2} = 0.9.$$

First, we use our numerical method to test stability without diffusion. Equations

$$u_t = \gamma(0.1 - u + u^2 v) \tag{56}$$
$$u_t = \gamma(0.9 - u^2 v) \tag{57}$$

with perturbed initial conditions give solutions $u = 1 = u^*, v = 0.9 = v^*$ at $t = 4$. Confirming the theory that $(u, v) = (1, 0.9)$ is a linearly stable uniform steady state solution (see figure (2)).

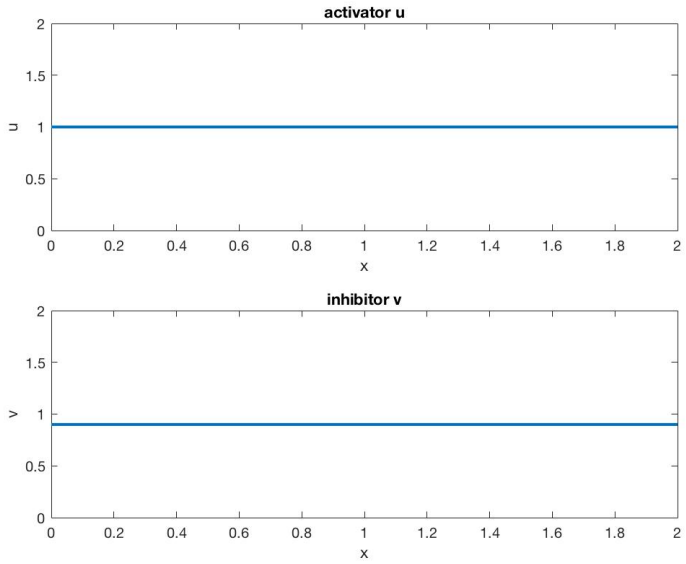

Figure 2: L = 10, a = 0.9, b = 0.1, t = 4

Now, we include the diffusion terms in the Schnakenberg model with parameters $\gamma = 197$ and $d = 40$, which satisfy the conditions for diffusion-driven instability in the linear stability analysis, and run numerical simulation. Patterns are generated after a short time. Figure (3) plot the concentrations of activator u and inhibitor v at time $t = 4$ and figure (4) captures the process of 1D pattern formation from $t = 0$ to $t = 4$.

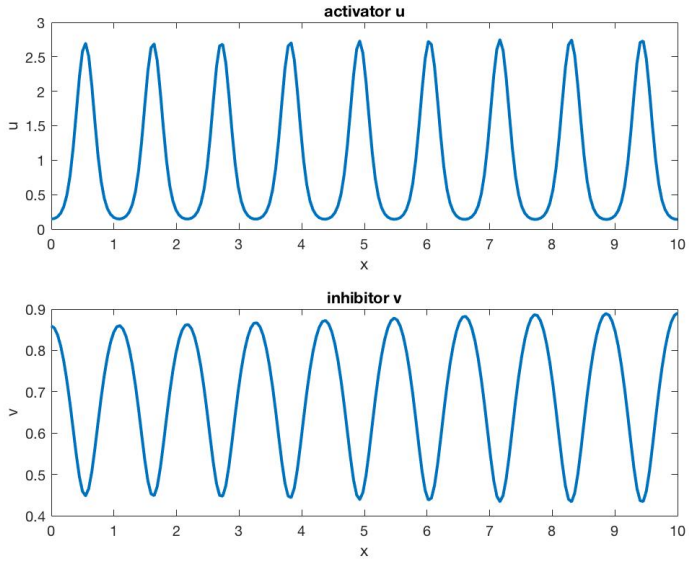

Figure 3: L = 10, a = 0.9, b = 0.1, d = 40, t = 4

4.2 Two-dimensional Schnakenberg

Now we consider nondimensionalised Schnakenberg model in 2D:

$$u_t = \gamma(a - u + u^2 v) + \nabla^2 u \tag{58}$$

$$v_t = \gamma(b - u^2 v) + d\nabla^2 v \tag{59}$$

for $(x, y) \in \Omega = [0, L_x] \times [0, L_y]$ and $t \in [0, \infty]$. Also, u, v satisfy no flux boundary conditions on $\partial\Omega$, and when $t = 0$, u and v are the randomly perturbed version of the steady state solutions.

Hence, the equation

$$\nabla^2 p + k^2 p = 0, \quad \mathbf{x} \in \Omega \tag{60}$$

$$\mathbf{n} \cdot \nabla p = 0, \quad \mathbf{x} \in \partial\Omega \tag{61}$$

gives us eigenfunction solutions

$$p_{m,n}(\mathbf{x}) = A_{m,n} \cos(m\pi x/L_x)\cos(n\pi y/L_y), \quad m, n = 0, 1, 2, \cdots \tag{62}$$

with corresponding

$$k_{m,n}^2 = \left(\frac{m\pi}{L_x}\right)^2 + \left(\frac{n\pi}{L_y}\right)^2 \quad \text{[3, p389].} \tag{63}$$

In the absence of diffusion, the two-dimensional Schnakenberg model has uniform steady-

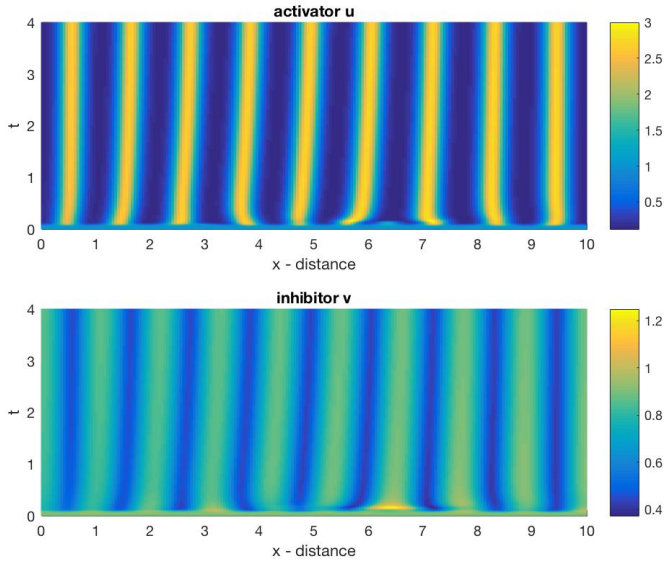

Figure 4: L = 10, a = 0.9, b = 0.1, d = 40, t = 4

state given by

$$u^* = a + b, \quad v^* = \frac{b}{(a+b)^2}$$

and has conditions for diffusion-driven instability (22), (23), (27) and (28).

4.2.1 Domain size and shape

In the two-dimensional case, the size and shape of the domain play an essential role in the generation of patterns. According to Murray, suppose we have a relatively small rectangular domain, i.e. L_x and L_y are small, and if

$$k_{1,1}^2 = \left(\frac{\pi}{L_x}\right)^2 + \left(\frac{\pi}{L_y}\right)^2 \notin [{k_-}^2, {k_+}^2],$$

diffusion-driven instability does not occur and patterns cannot be produced; if we consider a long and narrow rectangular domain, i.e. $L_x \ll L_y$, then, to create the environment for diffusion-driven instability ($k_{m,n} \in [{k_-}^2, {k_+}^2]$), we need $n = 0$ and thus there is no spatial heterogeneity in the x direction. Spatial variation evolves in only y direction, which results in stripe-looking patterns.

If we assume the domain is a sufficiently large rectangle, spatial inhomogeneous patterns evolve in both x and y directions, which result in spot-like patterns [3, p439-441].

4.2.2 Numerical results

To simulate the two-dimensional Schnakenberg model numerically, we let

$$u = u_0 + u^*, \quad v = v_0 + u^*,$$

where initial data u_0 and v_0 are the perturbed steady state solutions. Then, the reaction-diffusion equations can be written as:

$$\frac{\partial u^*}{\partial t} = \gamma(a - (u_0 + u^*) + (u_0 + u^*)^2(v_0 + v^*)) + \nabla^2 u^* \tag{64}$$

$$\frac{\partial v^*}{\partial t} = \gamma(b - (u_0 + u^*)^2(v_0 + v^*)) + \nabla^2 v^*. \tag{65}$$

To solve the equations, we adopt the numerical method introduced in Kristiansen's paper "Reaction-Diffusion Models in Mathematical Biology"[4, p63-64]. Specifically, we use Chebysehv interpolation to approximate the laplacian terms to converts the PDEs to a system of ODEs in time, which can be solved via MATLAB's build-in ode solver `ode15s`.

Firstly, we choose parameters a, b, and γ that satisfy conditions for diffusion-driven instability, and let the domain be a square with length $L_x = L_y = \pi$. The numerical results are shown in figure (5), where spotted patterns are present. They are consistent with the previous theory that a sufficiently large domain produces an environment for patterning in both x and y directions.

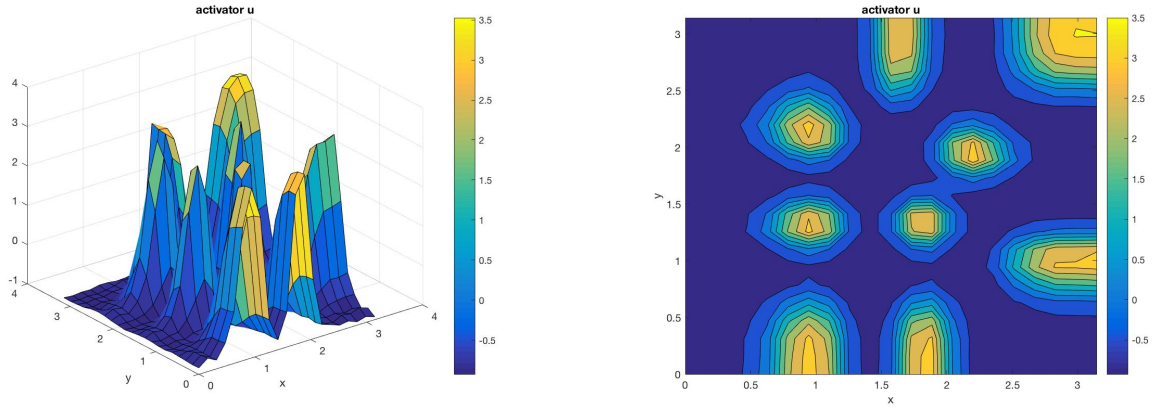

(a) 1 (b) 2

Figure 5: $L_x = L_y = \pi$, a = 0.9, b = 0.1, d = 40, t = 100

Secondly, we halve the length of the square domain so that $L_x = L_x = \pi/2$ and carry out the same numerical test holding other parameters constant. In figure (6), we observe a reduced number of spot patterns.

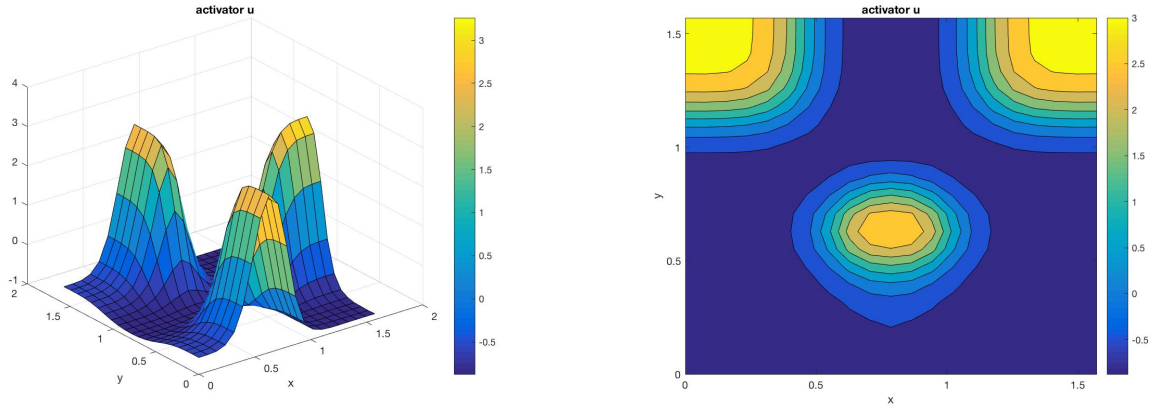

(a) 1 (b) 2

Figure 6: $L_x = L_y = \pi/2$, a = 0.9, b = 0.1, d = 40, t = 100

Thirdly, we create a long and nerrow domain by setting $L_x = \pi/2$ and $L_y = \pi/10$ while holding a, b, and γ constant. The numerical results in figure (7) display a stripped pattern, meaning that there is no spatial variation in the x direction.

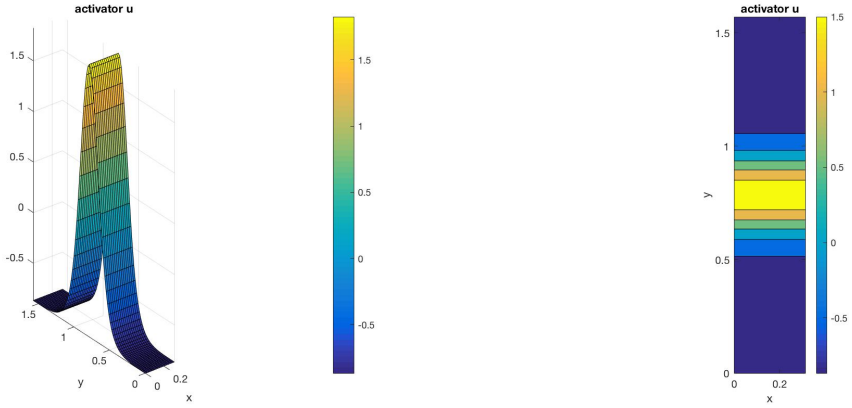

(a) 1 (b) 2

Figure 7: $L_x = \pi/2, L_y = \pi/10$, a = 0.9, b = 0.1, d = 40, t = 100

The predictions from the numerical results match the observation that animals tend to have stripe-like patterns on their tails which can be considered long and narrow domains and spot-like patterns on the rest of their bodies where the domains are large enough to produce patterns in two directions.

5 Conclusion and further work

In this paper, we have studied the influence of domain size and shape on pattern formation analytically and simulated pattern growths numerically on one-dimensional and two-dimensional domains with varying sizes and shapes. Regardless of the model dimensions, Turing mechanism fails to produce patterns if the size of the domain is too small, and patterns occur with a sufficiently large domain size. With parameters that admit diffusion-driven instability, we have numerically solved 1D and 2D Schnakenberg systems and confirmed that patterns appear in both cases provided the domains are sufficiently large. On a two-dimensional rectangular domain, the linear analysis predicts stripe-like patterns when the shape of the domain is long and narrow (with small width) and spot-like patterns when the length and width are both large. The numerical results are consistent with the analytic predictions and common observations in animal coat markings.

However, the paper only discusses pattern formation on spatial domains with simple geometries. For further work, we can adopt Turing models on more realistic domains with complex geometries. Moreover, the Schnakenberg model discussed in this paper is hypothetical. In future, we can also study other types of Turing models such as Gierer-Meinhardt model which is phenomenological and Thomas model which is empirical [1, p5]. Lastly, in developmental biology, it is more practical to investigate pattern formation on a growing domain instead of a fixed domain. Another extension of this paper is to study the impact of domain growth on diffusion-driven instabilities and pattern generation.

References

[1] Madzvamuse, A. (2000). *A Numerical Approach to the Study of Spatial Pattern Formation*, *D Phil Thesis*, University of Oxford.

[2] Madzvamuse, A., Thomas, R. D. K., Maini, P.K., and Wathen, A. J. (2002). A Numerical Method to the Study of Spatial Pattern Formation in the Ligaments of Arcoid Bivalves. *Bull. Math. Bio.* **64**, 501 - 530.

[3] Murray, J. D. (1989). *Mathematical Biology*, Biomathematics Vol. 19. Springer-Verlag, Heidelberg NY

[4] Kristiansen, K. (2008), Reaction-Diffusion Models in Mathematical Biology